International Journal of ChemTech Research
CODEN (USA): IJCRGG ISSN: 0974-4290
Vol.8, No.6, pp 203-215, 2015

The spectroscopic (FTIR, FT-Raman and UV), first-order hyperpolarizability and HOMO–LUMO analysis of an Antibiotic drug.

J.Sherin Percy Prema Leela[1*], R.Hemamalini[2] and S. Muthu[3]

[1]Department of Electronic Science, JBAS College for women, Tamilnadu, India
[2]PG & Research Department of Physics, Queen Mary's College, Tamilnadu, India
[3]Department of Physics, Sri Venkateswara College of Engineering, Sriperumpudur-602105, Tamilnadu, India

Abstract: The solid phase FTIR and FT-Raman spectra of Chloramphenicol (CLP) have been recorded in the regions 400-4000cm^{-1} and 100–4000cm^{-1}, respectively. The structure of the molecule was optimized and the structural characteristics were determined by density functional theory (B3LYP) method with 6-311++G(d,p) as basis set. UV–Visible spectrum of title compound was recorded in the region 200–800 nm and the electronic properties HOMO and LUMO energies were measured by time-dependent TD-DFT approach. Nonlinear optical properties like the dipolemoment, polarizability, first static hyperpolarizability, and molecular electrostatic potential surface have been calculated to get a better cognizance of the properties of the title molecule.Complete NBO analysis was alsocarried out to find out the intramolecular electronic interactions and their stabilisation energy. Also thermodynamic properties were interpreted. All the computed values are well agreed with the experimental data.

1 Introduction

Chloramphenicol(2,2-dichloro-N-[1,3-dihydroxy-1-(4-nitrophenyl)propan-2-yl]acetamide) is an antibiotic useful for the treatment of a number of bacterial infections and was shown to be effective against typhoid[1]. Chloramphenicol, also known as chlornitromycin, is effective against a wide variety of Gram-positive and Gram-negative bacteria. Synergistic activity of Salvia officinalis and Cichoriumintybus extracts and commonly used antibiotics, amoxicillin and chloramphenicol, were evaluated[2].Synergistic interactions were observed between amoxicillin and acetone or ethyl acetate extract of Salvia officinalis and between chloramphenicol and ethyl acetate extract of Salvia officinalis.The chemical formula is $C_{11}H_{12}Cl_2N_2O_5$. Oily chloramphenicol is recommended by the World Health Organization as the first-line treatment of meningitis. It was first used to treat meningitis [3]. Chloramphenicol is still widely used in topical preparations (ointments and eye drops) for the treatment of bacterial conjunctivitis[4]. In this work, we set out experimental and theoretical investigation of the vibrational and electronic transitions of Chloramphenicol(CLP). A detailed comment of the vibrational spectra of CLP has been made on the basis of the calculated potential energy distribution (PED). Literature survey reveals that so far there is no complete theoretical study for the title compound CLP. The redistribution of electron density (ED) in various bonding, antibonding orbitals and E(2) energies have been calculated by natural bond orbital (NBO) analysis to give clear evidence of stabilization originating from the hyper conjugation of various intra- molecular interactions. In the ground state theoretical geometrical parameters, HOMO and LUMO energies, thermodynamic properties of the title compound at different temperatures of were also calculated. The first order hyper polarizability (β_{total}) of this molecular system and

related properties (β, μ, and Δα) are calculated using B3LYP/6-311++G(d,p)methods based on the finite-field approach. All the calculations were performed using the Gaussian 03 program.

2 Experimental

The compound Chloramphenicol(2,2-dichloro-N-[1,3-dihydroxy-1-(4nitrophenyl)propan-2-yl]acet amide) in the solid form was purchased from the Sigma–Aldrich Chemical Company (USA) with a stated purity of 98% and used as such without furtherpurification. The FT-IR spectrum of the sample is recorded in the region 400–4000 cm^{-1} in evacuation mode using Bruker IFS 66V Spectrometer and FT-Raman spectrum of the molecule is recorded in the region 100–4000cm^{-1}in pure mode using Nd:YAG laser of 150mW on a BRUKER RFS 100/s at SAIF, IIT and Chennai, India. The observed experimental and stimulated FTIR andFT-Raman spectra are shown in Figures 2 and 3, respectively. The ultraviolet absorption spectrum has been recorded using a Perkin Elmer lambda 35 spectrophotometer in the range of 200-800nm are shown in Fig 6.

3. Computational details

The entire calculations were performed at density functional (DFT) levels on a Pentium IV personal computer using Gaussian03program[5] package invoking gradient geometry optimization. The harmonic vibrational frequencies were calculated at the same level of theory for the optimized structures and obtained frequencies were scaled by 0.961[6].Next the spectra were analyzed in terms of the Potential Energy Distribution (PED) contributions by using the Vibrational Energy Distribution Analysis Program [7].The Raman activities (S_i) calculated by Gaussian 03 program have been suitably adjusted by the scaling procedure with MOLVIB and subsequently converted to relative Raman intensities (I_i) using the following relationship derived from the basic theory of Raman scattering[8].

$$I_i = \frac{f(\upsilon_0-\upsilon_i)^4 S_i}{\upsilon_i [1 - \exp (hc\upsilon i/k_bT)]}$$

Where $\upsilon_0$is the exciting frequency (in cm^{-1}), υ_i is the vibrational wave number of the ith normal mode, h, c and k_b are universal constants, and f is the suitably chosen common scaling factor for all the peak intensities. For the plots of simulated IR and Raman spectra, pure Lorentzian band shapes are used with full width at half maximum of 10 cm^{-1}. The natural bond orbital (NBO) calculations [9] were performed using NBO 3.1 program as implemented in the Gaussian 03W package at the above said level. In order to understand various second order interactions between the filled orbital of one subsystem and vacant orbital of another subsystem. This is a measure of the inter-molecular and intra-molecular delocalization or hyper conjugation.UV–Vis spectra, electronic transitions, vertical excitation energies, absorbance and oscillator strengths were computed with the time-dependent DFT method. To investigate the reactive sites of the title compound the MEP were evaluated using the B3LYP/6-31G(d,p) method. The mean linear hyperpolarizability and mean first hyperpolarizability properties of the title compound were obtained molecular polarizabilities based on theoretical calculations [10].

4. Results and discussion

4.1Optimized geometry

The optimized structural parameters (bond length and bond angle) of CLP were also calculated by DFT/B3LYP with 6-311++G(d,p) basis set, which are presented in Table 1. The atom numbering scheme adopted in this study is given in Figure 1.

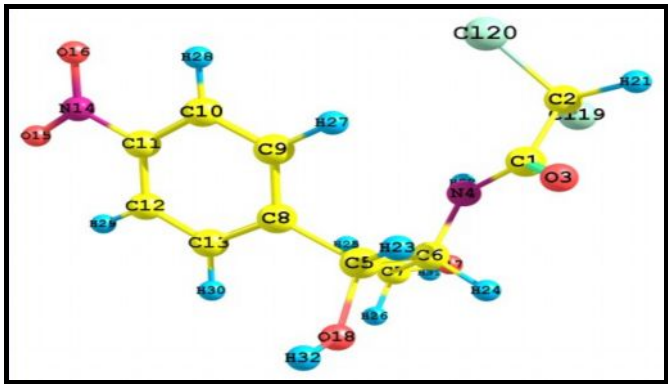

Fig1. The structure of Chloramphenicol predicted by the B3LYP/6-311++G(d,p) level.

This molecule has ten C-C bond lengths, three C-O bond length, one N-H bond lengths, two C-N bond lengths, nine C-H bond lengths, O-H three bond lengths and two C-Cl bond length. The calculated geometric parameters can be used as foundation to calculate the other parameters for the compound.

Table.1. Optimized geometrical parameters of Chloramphenicol molecules, bond length (Å), bond angles (°).

Bond length	Value	Bond Angle	Value
C1-C2	1.541	Cl20-C2-H21	106.9
C1-O3	1.22	C6-N4-H22	115.7
C1-N4	1.35	N4-C6-C5	112.8
C2-Cl19	1.801	N4-C6-C7	108.5
C2-Cl20	1.803	N4-C6-H24	108.7
C2-H21	1.084	N4-H22-O17	101.3
N4-C6	1.464	C6-C5-C8	114.9
N4-H22	1.012	C6-C5-O18	104.6
C5-C6	1.556	C6-C5-H23	106
C5-C8	1.521	C5-C6-C7	112.6
C5-O18	1.43	C5-C6-H24	105.4
C5-H23	1.093	C8-C5-O18	112.3
C6-C7	1.525	C8-C5-H23	108.7
C6-H24	1.095	C5-C8-C9	119.8
C7-017	1.43	C5-C8-C13	121.2
C7-H25	1.097	O18-C5-H23	110.1
C7-H26	1.093	C5-O18-H32	108.9
C8-C9	1.4	C7-C6-H24	108.6
C8-C13	1.4	C6-C7-O17	107.1
C9-C10	1.39	C6-C7-H25	110.2
C9-H27	1.083	C6-C7-H26	108.6
C10-C11	1.391	O17-C7-H25	110.3
C10-H28	1.081	O17-C7-H26	111.6
C11-C12	1.391	C7-O17-H31	109.1
C11-N14	1.478	C7-O17-H22	77.3
C12-C13	1.39	H25-C7-H26	109
C12-H29	1.081	C9-C8-C13	119
C13-H30	1.083	C8-C9-C10	120.9
N14-015	1.225	C8-C9-H27	120
N14-O16	1.225	C8-C13-C12	120.8
O17-H31	0.962	C8-C13-H30	119.4
O18-H32	0.962	C10-C9-H27	119.1
O17-H22	2.338	C9-C10-C11	118.7
		C9-C10-H28	121.6
		C11-C10-H28	119.8
Bond Angle	**Value**	C10-C11-C12	121.8
C2-C1-O3	117.9	C10-C11-N14	119.1
C2-C1-N4	116.9	C12-C11-N14	119
C1-C2-Cl19	113.7	C11-C12-C13	118.7
C1-C2-Cl20	109.8	C11-C12-H29	119.7
C1-C2-H21	107.8	C11-N14-O15	117.7
O3-C1-N4	125.2	C11-N14-O16	117.7
C1-N4-C6	122.3	C13-C12-H29	121.6
C1-N4-H22	117.4	C12-C13-H30	119.8
Cl19-C2-Cl20	111	O15-N14-O16	124.6
Cl19-C2-H21	107.4	H31-O17-H22	136.8

Inclusion of CH group and NH atoms known for its strong electron-withdrawing nature, is expected to increase a contribution of the resonance structure, in which the electronic charge is concentrated at this site. This is the reason for the shortening of bond lengths N11–H12 = 1.012 Å,C2-H21= 1.084Å obtained by DFT method compared to other bond length. In this title molecule the bond angle C7-O17-H22 = 77.3˚ are appreciably smaller than the other C5-O18-H32 = 108.9˚ and C7-O17-H3 = 109.1˚ calculated by DFT/B3LYP with 6-311++G(d,p) basis set method.

4.2Vibrational spectra analysis

The vibrational spectrum is mainly determined by the modes of the free molecule observed at higher wavenumbers, together with the lattice (translational and vibrational) modes in the low wavenumber region. The observed experimental FT-IR and FT-Raman spectra along with the theoretical spectra are shown in Figs. 2-3.

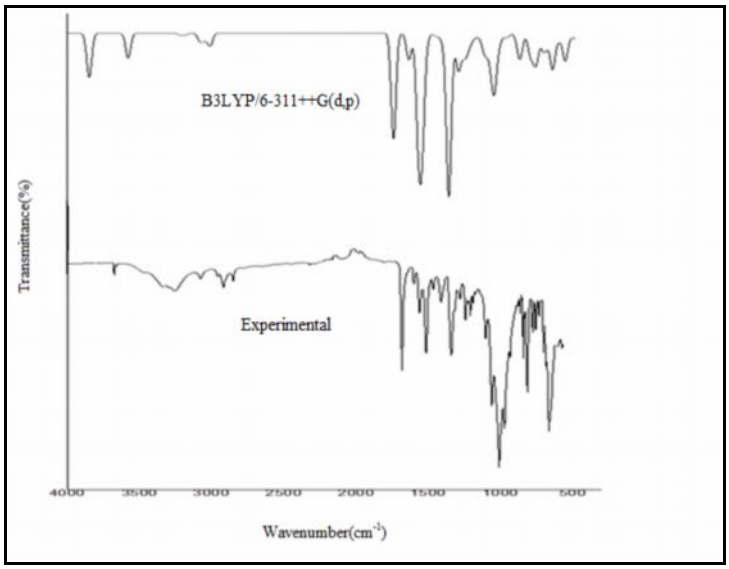

Fig 2. Experimental and theoretical FTIR spectra of Chloramphenicol(CLP)

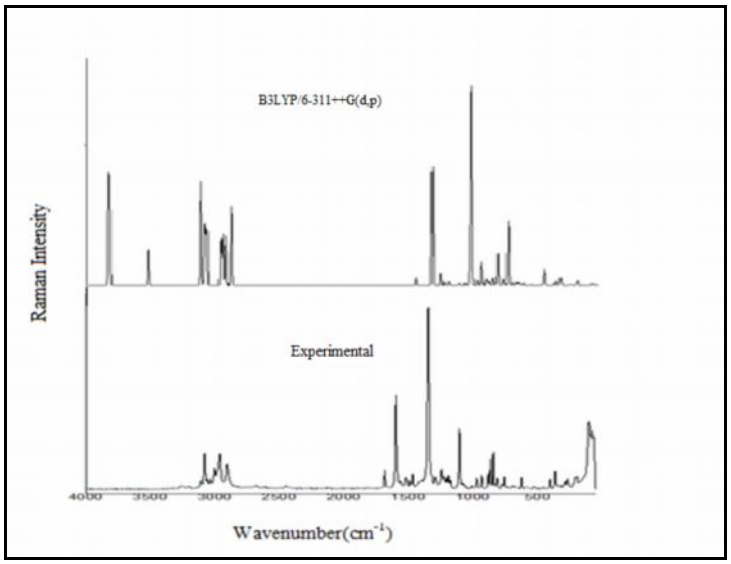

Fig 3. Experimental and theoretical FT-RAMAN spectra of Chloramphenicol(CLP)

In order to obtain the spectroscopic signature of the CLP molecule, we performed a frequency calculation analysis. Calculations were made for a free molecule in vacuum, while experiment swere performed for solid sample; therefore, there are disagreements between calculated and observed vibrational wavenumbers. After applying the different scaling factors, the theoretical wavenumbers are in good agreement with experimental wavenumbers. Vibrational frequencies were calculated by using B3LYP/6-311++G(d,p) for the title molecule having 32 atoms with 90 normal modes. The experimental and theoretical vibrational wavenumbers of CLP and their assignments using PED are given in Table 2.

4.2.1 N–H stretching

The heteroaromatic structure shows the presence of N–H stretching vibrations above 3000 cm^{-1}which is the characteristic region for ready identification of this structure [11].The frequencies of the amino group appear around 3500–3300 cm^{-1} for the NH2 stretching and bands in the range 1630–1610 cm^{-1} due to N-H in-plane deformation [12]. In the present case the bands observed at 3468 cm^{-1} in the IR spectrum and theoretically these N- H stretching modes are observed at 3439 cm^{-1} with a large contribution of 97% PED. The bands for N–H in-plane bending vibrations of the title compound are identified at 1550 cm^{-1} in FT-IR spectra which shows good agreement with the computed B3LYP/6-311++ G(d,p) result.

4.2.2 C=O vibrations

Table 2.Experimental and calculated DFT-B3LYP/6-311++G(d,p) levels of vibrational frequencies (cm^{-1}) of Chloramphenicol.

Experimental wave number $(cm)^{-1}$		Frequencies cm^{-1}	FT-IR		FT-Raman		Assignment of vibrational modes			
FT-IR	FT-Raman	scaled	Relative	Absolute	Relative	Absolute				
		3701	57	17	140	80	γOH(52)	βHOC(13)	τHOCC(30)	
		3693	57	17	111	63	γOH(26)	βHOC(62)		
3468		3439	63	19	51	29	γNH(97)			
3267	3110	3097	3	1	71	41	βHCC(76)			
	3081	3095	2	0	82	47	γCH(15)	βHCC(31)	τHCCC(26)	
	3037	3070	1	0	46	26	γCH(10)	βHCC(18)	βHCC(27)	τHCCC(17)
		3064	2	1	65	37	βHCC(45)			
3010	3005	3055	2	1	77	44	βHCC(13)	βHCCI(14)	τHCCC(11)	OUT CCCH(12)
		2962	18	6	67	38	τHCCC(49)			
		2949	3	1	73	42	τHCCC(11)	OUT CCCH(54)		
2923		2929	13	4	71	41	βHCC(30)	τHCNC(18)		
2854	2963	2895	32	10	113	65	γCH(26)	βHCO(11)	τHCCC(29)	
1701	1685	1681	265	81	12	7	γOC(71)			
	1599	1580	51	16	2	1	γCC(11)	βONC(12)	βNCC(10)	
1534	1520	1574	16	5	169	97	γCC(22)	βCCC(24)		
		1516	242	74	17	10	γON(25)	βONC(24)		
1550	1491	1492	257	78	4	2	βHNC(19)	τHNCC(51)		
		1465	11	3	3	2	βCCC(15)			
1463	1468	1462	10	3	3	2	γCH(58)	βHCO(17)		
1378	1348	1399	3	1	1	1	γCH(28)	βHCH(16)		
		1396	4	1	3	2	γCH(12)	βHCH(16)		
		1356	19	6	3	2	γCH(17)			
1323	1303	1329	1	0	18	10	γCH(22)	βHCC(11)	βONO(15)	
		1318	83	25	175	100	βHCC(34)			
		1314	328	100	156	89	γCH(33)	βONO(25)		
		1297	4	1	1	0	βNCC(12)			
		1277	14	4	7	4	γCH(24)			
		1250	79	24	27	15	γCH(10)			
1236	1245	1223	13	4	9	5	γCH(14)	βHCCI(10)	OUT CCICH(15)	
	1228	1214	20	6	3	2	γCH(32)	βHCCI(16)	OUT CCICH(20)	
	1210	1202	20	6	5	3	γCC(13)	βHCCI(16)	OUT CCICH(14)	OUT CICCICH(16
	1192	1198	17	5	1	1	γCH(11)	βHOC(10)		
1164	1176	1174	22	7	11	6	βHOC(15)	βHCC(19)		
		1154	2	1	3	2	γCC(14)			
	1107	1106	11	3	10	5	γNC(11)			
		1074	46	14	92	53	γCH(12)	γNC(13)		
		1045	39	12	4	2	βCCN(18)			
		1021	88	27	4	2	γOC(11)	OUT OCCC(38)		
1031		1008	66	20	4	2	γOC(13)	βOCC(47)	OUT OCCC(11)	
		991	14	4	2	1	γCC(27)			
920	974	972	11	3	3	2	γCH(11)	βHCC(13)	τHCCC(88)	
	935	970	2	1	0	0	τHCCN(13)			
850	883	848	31	9	1	1	βHCO(13)			
	865	837	34	10	23	13	τHCCN(10)	τHCCC(27)		
	845	826	0	0	1	0	γON(33)			
	816	777	39	12	3	2	βOCN(17)	OUT OCNC(11)	OUT CICCIC(14)	
722	759	761	26	8	7	4	γCIC(13)	βCICC(14)		
		738	50	15	4	3	OUTOCON(17)			
		689	38	12	0	0	γON(15)	OUT OCON(23)		
	626	626	90	27	3	2	βCICCI(24)	τCCNC(10)		
605		586	18	6	1	0	γCC(22)	τCCCC(17)		
		544	68	21	1	0	βHNC(59)	τHNCC(28)		
		523	4	1	2	1	βCCC(10)			
		501	8	3	1	1	βCCC(14)	βNCC(11)	βCCC(13)	
		447	2	1	1	0	γNC(13)			
	404	406	0	0	0	0	τCCCC(25)	τCCCC(12)		
	365	395	5	1	6	3	γCIC(14)	βCCN(18)	τCICCN(17)	
		332	4	1	1	1	βCNC(10)			
		301	8	2	2	1	γCC(10)	βCNC(10)		
	285	280	61	19	2	1	βCCN(14)	τHOCC(16)		

Abbreviations-γ-stretching;β-bending;τ-Torsion,inp-planebending,opb-out of plane bending. Absolute-absorption intensity. Relative -absorption intensities normalized with highest peak absorption equal to 100.

The carbonyl stretching frequency has been most extensively studied by infrared spectroscopy[13]. This multiple bonded group is highly polar and therefore gives rise to an intense infrared absorption band. In the present study the carbonyl-stretching vibrations[14] are found in the region of 1780–1700 cm^{-1}. In our present study, the strong band 1701cm^{-1}in FT-IR spectra and band 1685cm^{-1} in FT-RAMAN are assigned to C=O stretching vibration shows small deviation calculated byB3LYP/6-311++ G(d,p) method at 1681 $cm^{-1}$and with71% of PED contribution.

4.2.3 C–C vibrations

There are six equivalent C–C bonds in benzene and consequently there will be six C–C stretching vibrations. In addition, there are several in-plane and out-of-plane bending vibrations of the ring vibrations. However, due to high symmetry of benzene, many modes of vibrations are infrared inactive.I n general the bands around 1400–1650 cm^{-1} in benzene derivatives are assigned to C–C stretching vibrations [15].In the title compound the FT-IR bands of C–C stretching is found at 1534 cm^{-1}.The Raman bands of C–C stretching of the pyridine ring appear at 1599 and 1520 cm^{-1}. These assignments are in good agreement with the calculated at 1574cm^{-1} byB3LYP/6-311++ G(d,p) method.

4.2.4 C-H vibrations

The C-H stretching vibrations are normally observed in the region above 3000 $cm^{-1}$for the benzene and less than 3000 $cm^{-1}$for non-aromatic compounds [16]and pyrazole compounds[17]. The aromatic structures shows the presence of C-H stretching vibrations in the region 3100–3000 cm^{-1} which is the characteristic region for the ready identification of C-H stretching vibrations[18].In our case C-H stretching vibrations observed at 3081cm^{-1} and 3037cm^{-1}in FT-Raman spectrum. The calculated wavenumbers at the range 3095$cm^{-1}$and 3070cm^{-1}assigned C-Hstretching vibrations, which is good agreement with experimental . The C-H stretching vibrations observed at 2854cm^{-1}in FT-IR and 2963cm^{-1}in FT-Raman spectrum. The calculated wavenumbers at the range 2895cm^{-1}assigned C-Hstretching vibrations, which is good agreement with experimental values and PED contributes almost above 26%. The bands due to C-H in-plane ring vibration interacting with C-C stretching vibrations and are observed in the region 1000–1300 cm^{-1}which reflects the characteristics of the molecule [19]. In this study, the C–Hin-plane-bending vibrations observed at 1378,1323,1236 and 1164 cm^{-1}in FT-IR the bands observed at 1348,1303,1245,1228,1210,1192 and 1176 in FT-Raman. which shows good agreement with calculated frequencies and the modes gives major PED contribution of above10% respectively. The aromativity of the compound obviously proved by the presence of the strong peak below 900 $cm^{-1}$and the substitution patterns on the ring can be judged from the out of plane bending of the ring C-H bond in the range of 900–675 cm^{-1}which are more informative [20]. In the present study, the peaks at 920 and 850 cm^{-1} in FT-IR and 974 and 823 cm^{-1}in FT-Raman and the calculated frequency at 972 and 848 cm^{-1},bothconfirm the C-H out of plane bending vibrations which agree well with the above said literature values.

4.2.5 C–Cl vibrations

The vibrations belonging to C–X (X = F, Cl, Br) bonds which are formed between the ring and the halogen atoms, are interesting. Since mixing of vibrations is possible due to the lowering of molecular symmetry and the presence of heavy atoms [21]. Generally, the C-Cl absorption is obtained in the broad region between 850 and550cm^{-1}[22]. Therefore, the band found at 759 cm^{-1} in the FT-Raman spectra has been designated to C-Cl stretching mode of vibration with 13% PED contribution and it shows good agreement with the theoretical wave number of C–Cl stretching vibration 761cm^{-1} by B3LYP/6-311++G(d,p) coincides very well with the experimental value.

4.3 NBO

Natural bond orbital (NBO) analysis presents an efficient method for studying interesting features of molecular structure. It gives a strong insight in the intra and intermolecular bonding and interaction among bonds. Also, it provides a convenient basis for investigating charge transfer in molecular system[23] .The filled NBOs of the natural Lewis structure are well adopted to describe covalency effects in molecule. The anti-bonds represent empty valence-shell capacity and spanning portions of the atomic valence space that are formally unsaturated by covalent bond formation. In order to understand various second order interactions between the filled orbitals of one subsystem and vacant orbitals of another subsystem, which is a measure of the

delocalization or hyperconjugation. The hyperconjugative interaction energy was deduced from the second order perturbation approach[24].For each donor (i) and acceptor (j), the stabilization energy E $^{(2)}$ associated with the delocalization i → j is estimated as

$$E^{(2)} = \Delta E_{ij} = \frac{q_i(F_{ij})^2}{\varepsilon_j - \varepsilon_i}$$

Where q_i is the donor orbital occupancy, ε_j and ε_i are diagonal elements and F_{ij} is the off diagonal NBO Fock matrix element. Some electron donor orbital, acceptor orbital and the interacting stabilization energy resulting from the second-order micro-disturbance theory are reported[25].In order to investigate the intra- and intermolecular interactions, the occupancy andthe stabilization energies of the title compound were performed using second-order perturbation theory calculated at B3LYP/6-311++G(d,p) are presented in Table 3.The larger the E(2) value, the more intensive is the interaction between electron donors and electron acceptors, i.e. the more donating tendency from electron donors to electron acceptors and the greater the extent of conjugation of the whole system. The intra-molecular interaction is formed by the orbital overlap between σ(C-C) and σ*(C-C) bond orbital which results intra-molecular charge transfer (ICT) causing stabilization of the system. These interactions are observed as increase in electron density (ED) in C-C, C-H, C-O and N-H antibonding orbital that weakens the respective bonds.

Table 3 Second order perturbation theory analysis of Fock matrix in NBO basis for Chloramphenicol.

Donor (i)	Type	ED/e	Acceptor (j)	Type	ED/e	[a]E(2) (kJ/mol)	[b]E(j) – E(i) (a.u)	[c]F(i,j)
C1-O3	σ	1.99157	N4-H22	σ*	0.02083	1.74	1.46	0.045
	π	1.98068	C2-Cl20	σ*	0.05684	2.88	0.47	0.033
	π*		C2-Cl20	σ*	0.05684	9.24	0.06	0.051
C2-Cl19	σ	1.98726	C1-N4	σ*	0.07154	3.9	1.13	0.06
C2-Cl20	σ	1.98168	C1-O3	π*	0.27357	3.01	0.71	0.044
C5-C8	σ	1.96927	C8-C9	σ*	0.02973	3.15	1.3	0.057
			C8-C13	σ*	0.03216	4.48	1.14	0.064
C7-H26	σ	1.9568	C8-C9	π*	0.31136	4.61	0.56	0.049
			C12-C13	π*	0.27754	7.15	0.55	0.06
C8-C13	σ	1.96248	C8-C9	σ*	0.02973	5.73	1.41	0.08
			C9-H27	σ*	0.02084	3.06	1.16	0.053
C9-C10	σ	1.97319	C5-C8	σ*	0.04384	4.09	1.17	0.062
			C8-C9	σ*	0.02973	5.94	1.4	0.081
C9-H27	σ	1.97552	C8-C13	σ*	0.03216	5.46	1.16	0.071
			C10-C11	σ*	0.03002	3.71	1.14	0.058
C10-C11	σ	1.96323	C11-C12	σ*	0.03023	8.9	1.37	0.099
			N14-O15	σ*	0.03513	4	1.38	0.066
	π	1.62066	C8-C9	π*	0.31136	16.71	0.33	0.067
C10-C11	π*	0.37103	C8-C9	π*	0.31136	310.47	0.01	0.093
			N14-O15	π*	0.58503	46.35	0.19	0.089
C10-H28	σ	1.9728	C8-C9	σ*	0.02973	4.3	1.17	0.063
			C11-C12	σ*	0.03023	4.56	1.14	0.064
C11-C12	σ	1.96151	C10-C11	σ*	0.03002	8.92	1.37	0.099
			N14-O16	σ*	0.09458	4.7	1.05	0.064
C11-N14	σ	1.98613	C10-C11	σ*	0.03002	3.9	1.57	0.07
			C11-C12	σ*	0.03023	3.21	1.56	0.063
C12-C13	σ	1.97158	C8-C13	σ*	0.03216	5.89	1.39	0.081
			C11-C12	σ*	0.03023	4.76	1.37	0.072
	π	1.6664	C7-H26	σ*	0.04976	6.06	0.67	0.061
			C8-C9	π*	0.31136	22.31	0.32	0.076
			C10-C11	π*	0.37103	20.75	0.31	0.072
C12-H29	σ	1.97334	C8-C13	σ*	0.03216	4.32	1.16	0.063
			C10-C11	σ*	0.03002	4.55	1.14	0.064
C13-H30	σ	1.97116	C8-C9	σ*	0.02973	5.43	1.17	0.071

			C11-C12	σ*	0.03023	3.75	1.14	0.058
N4-H22	σ	1.98634	C1-O3	σ*	0.01814	3.9	1.29	0.063
N14-O15	σ	1.99483	C11-N14	σ*	0.0765	3.38	1.76	0.07
	π	1.97912	C10-C11	π*	0.37103	7.52	0.53	0.062
	π*		C10-C11	π*	0.37103	33.11	0.12	0.082
N4	LP(1)	1.71427	C1-O3	π*	0.27357	58.85	0.29	0.117
O15	LP(2)	1.86983	N14-O16	σ*	0.09458	31.86	0.6	0.125
O16	LP(3)	1.5413	N14-O15	π*	0.58503	95.66	0.15	0.112
Cl19	LP(3)	1.94716	C2-Cl20	σ*	0.04485	8.37	0.4	0.051
Cl20	LP(3)	1.94823	C2-Cl19	σ*	0.05684	7.86	0.43	0.052

[a]$E^{(2)}$ means energy of hyper conjugative interaction (stabilization energy),[b]E(j) – E(i)Energy difference between donor and acceptor i and j NBO orbital's,[c]F(i,j) is the Fock matrix element between i and j NBO orbital's.

For example the delocalization of π electron from π (C8–C9) distribute σ*(C5-O18), π* (C10-C11), π* (C12-C13) leading to the stabilisation energy of 26.88 kJ/mol due to strong conjugative interactions .A very strong interaction has been observed due to the electron density transfer from the lone pair (LP1) of Nitrogen atom (N4) to antibonding orbitals π* (C1-O3) with stabilization energies 58.85 kJ/mol. In the case of LP2 of Oxygen atom (O15) and LP(3) of (O16) to the antibonding acceptor *σ*(N14-O16) and π*(N14-O15) has large stabilisation energy of 31.86 and 95.66kJ/mol as shown in Table 2. The lone pair of LP3 of Chlorine atom (Cl19) and LP(3) of (Cl20) to the antibonding acceptor *σ*(C2-Cl20) and π*(C2-Cl19) has stabilisation energy of 8.37 and 7.86 kJ/mol .The interaction energy, related to resonance in the molecule, is electron withdrawing from the ring through π*(C10-C11) of the NBO conjugated with π*(C8-C9) resulting with large stabilisation of 310.47 kJ/mol. Therefore, the maximum energy delocalization takes place in the π* – π* transition which quantity extend the intermolecular hydrogen bonding.

4.4 NLO

Table 4. The Electric dipole moments (Debye) μ, Polarizability α (in esu), βHyperpolarizability andβtot (10^{-30}esu) value ofChloramphenicol calculated by B3LYP/6-311++G(d,p) method.

Parameters	B3LYP/6-311++G(d,p)	Parameters	B3LYP/6-311++G(d,p)
μ_x	-0.0462438	β_{xxx}	1155.644798
μ_y	0.224165	β_{xxy}	-559.350854
μ_z	0.9615104	β_{xyy}	258.6631891
μ (D)	0.9883778	β_{yyy}	48.8768101
α_{xx}	226.7355311	β_{xxz}	-198.004854
α_{xy}	-41.7935507	β_{xyz}	62.8752356
α_{yy}	201.36902	β_{yyz}	6.0950855
α_{xz}	-16.0309556	β_{xzz}	18.8188418
α_{yz}	0.6410626	β_{yzz}	27.6220834
α_{zz}	149.6384413	β_{zzz}	23.4006469
$\alpha_{(a.u)}$	192.5809975	β_{tot} (esu)	1.3146×10^{-29}
Δα (esu)	2.8541×10^{-23}		

Nonlinear optical (NLO) effects arise from the interactions of electromagnetic fields in various media to produce new fields altered in phase, frequency, amplitude or other propagation characteristics from the incident fields [26]. Organic materials are molecular materials that consist of chemically bonded molecular units interacting in the bulk media through weak van-der Waal interactions and possess ease of fabrication and integration into devices, relatively low cost, fast response, intrinsic tailorability which is responsible for NLO properties[27]. Nonlinear optics[28] is given increasing attention due to its wide application in the area of laser technology, optical communication and data storage technology. NLO properties like the dipole moment, polarizability, first static hyperpolarizability have been calculated using B3LYP/6-311++G(d,p) to get a better cognizance of the properties of the title molecule and their calculated values are given in Table 4.

The complete equations for calculating the magnitude of total static dipole moment μ, the mean polarizability α, the anisotropy of the polarizability Δα and the mean first polarizability β, using the x, y, z components from Gaussian 03W output is as follows:

$\mu_{tot} = (\mu^2_x + \mu^2_y + \mu^2_z)^{1/2}$
$\alpha = 1/3(\alpha_{xx} + \alpha_{yy} + \alpha_{zz})$
$\Delta\alpha = 2^{-1/2}[(\alpha_{xx} - \alpha_{yy})^2 + (\alpha_{yy} - \alpha_{zz})^2 + (\alpha_{zz} - \alpha_{xx})^2 6\alpha^2_{xx}]^{1/2}$
$\beta_{\mu tot} = (\mu_x + \mu_y + \mu_z)$ and
$\beta_x = \beta_{xxx} + \beta_{xyy} + \beta_{xzz}$
$\beta_y = \beta_{yyy} + \beta_{xxy} + \beta_{yzz}$
$\beta_z = \beta_{zzz} + \beta_{xxz} + \beta_{yyz}$

The search for molecules possessing a large value of static first hyperpolarizability is a key step toward the optimization of new materials for NLO response applications. The total molecular dipole moment of CLP from DFT with 6-311++G(d,p) basis set is 1.20695 D, which are nearer to the value of urea (μ = 0.9884D). Similarly the first order hyperpolarizability of CLP with DFT/6-311++G(d,p) basis set is 1.3146×10^{-29}esu thirty five times greater than the value ($\beta = 0.372 \times10^{-30}$esu)[29]. Also, the NLO properties of a molecule are related to the energy gap between HOMO and LUMO. The B3LYP/6-311++G(d,p) calculated energy gap is E=4.8553eV which is lower than urea (ΔE = 6.7063 eV). Therefore, investigated molecule is suitable for non-linear optical applications.

4.5 Analysis of Frontier molecular orbitals (FMOs) and Molecular electrostatic potential

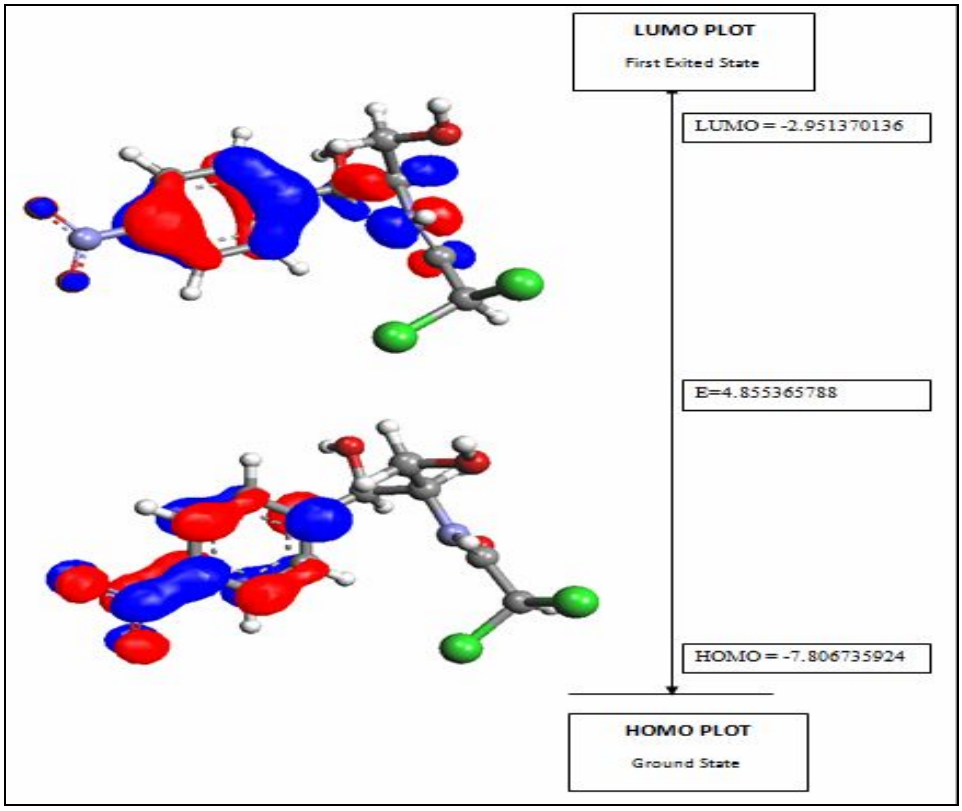

Fig 4. Highest occupied and Lowest unoccupied molecular orbitals of Chloramphenicol obtained by B3LYP/6-31++G(d,p) method.

The Frontier molecular orbital and their properties like energy are very useful to the physicists and chemists and their frontier electron density used for predicting the most reactive position in p-electron system and also explained several types of reaction in conjugated systems[30].The energy of the HOMO is directlyrelated to the ionization potential and characterizes the susceptibilityof the molecule toward attack of electrophiles. The energyof LUMO is directly related to the electron affinity[31]and characterizesthe susceptibility of the molecule toward attack of nucleophiles.The concept of hard and soft nucleophiles andelectrophiles has been also directly related to the relative energiesof the HOMO and LUMO orbitals. A molecule with a small frontier orbital gap is more polarizable and is generally associated with a high chemical reactivity, low kinetic stability and is also termed as soft molecule[32]. The HOMO–LUMO energy gap of Chloramphenicol(CLP) was calculated at the

B3LYP/6-311++G(d,p) . The positive and negative phase represented in red and blue colour, respectively are shown in Fig 4. The energy gap between HOMO and LUMO determines the kinetic stability, chemical reactivity and, optical polarizability and chemical hardness–softness of a molecule[33]. The calculated energy gap (4.8553eV) clearly indicates that the charge transfer takes place within the molecule, which increases the molecular activity of molecule.

The MESP is a physical property of a molecule related to how a molecule is first ‘‘seen’’ or ‘‘felt’’ by another approaching species.The molecular electrostatic potential (MEP) is relatedto the electronic density and is a very useful descriptor for determiningsites for electrophilic attack and nucleophilic reactions aswell as hydrogen-bonding interactions[34]. A portion of a molecule that has a negative electrostatic potential is susceptible to an electrophilic attack – the more negative the better.The electrostatic potential the space around a molecule by its nuclei and electrons (treated as static distributions of charge), is a very useful property to analyze and predict molecular reactive behavior. The different values of the electrostatic potential at the surface are represented by different colors. Potential increases in the order red < orange < yellow < green < blue. Fig 5 provides a visual method to understand the relative polarity of the titlemoleculewas calculatedat the B3LYP/6-311++G(d,p).

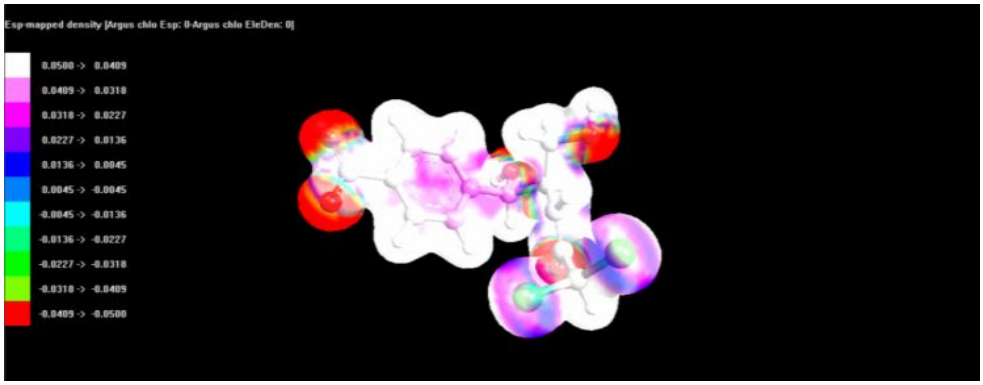

Fig 5.Molecular ElectrostaticPotential(MEP) of Chloramphenicol obtained by B3LYP/6-31++G(d,p) method.

In MEP, maximum negative region represents the site for electrophilic attack indicated by red color while the maximum positiveregion represents nucleophilic attack indicated in blue color. As can be seen from the MEP map of the title molecule, while regions having the negative potential are over the electronegativeatom (Oxygen and Carbon atoms), the regions having the positive potential are over the hydrogen atoms.

4.6 Electronic absorption spectra

In order to understand electronic transitions in terms of energies and oscillator strengths, the TD-DFT calculations excited electronic states were performed in the gaseous phase[35]. The UV–Vis spectral analysis of CLP have been calculated by TD-B3LYP/6-311++G(d,p) CIS method along with measured UV–Visdata are summarized in Table 5.

Table 5 : The UV–Vis excitation energy and oscillator strength (f) for Chloramphenicol.

States	λobs (nm)	λcal (nm)	Excitation energy(eV)	Oscillator Strength(f)
S1	402.38	406.84	3.0475	0.0000
S2	360.70	327.90	3.7812	0.1268
S3	308.18	306.39	4.0466	0.0032

All the molecular structure allows strong π – π*or σ–σ*transition in the UV–vis region with a high extinction coefficients[36].The lowest singlet → singlet spin-allowed excited states weretaken into account to investigate the properties of electronicabsorption. The experimental UV spectra are shown inFigure6.

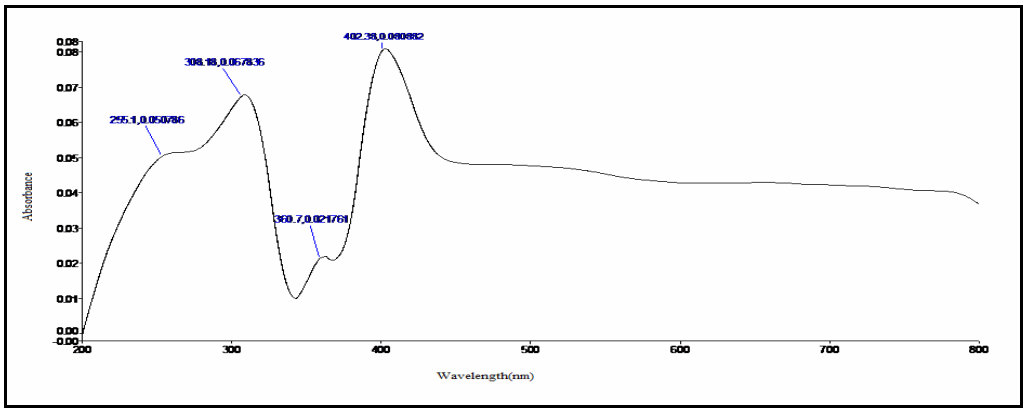

Fig 6. Experimental UV-vis spectra of Chloramphenicol (CLP)

Calculations involving the vertical excitation energies, oscillatorstrength (f) and wave length have been carried out and listedin Table 5. The calculations of molecular orbital geometry show that the visible absorptionmaxima of this molecule correspond to the electrontransition between frontier orbitals, such as translation fromHOMO to LUMO as can be seen from the UV vis spectra absorptionmaxima values have been found to be 402.38, 360.70 and308.18 nm are due to the $\pi - \pi^*$. The λ_{max} is a functionof substitution, the stronger the donor character of the substitution,the more electrons pushed into the ring, the larger λ_{max}. TD-DFT (B3LYP) with 6-311++G(d,p) predict one intenseelectronic transition at (λ_{max} = 40**6.**84nm) with a excitation energyE = 3.0475eV is good agreement with the measured experimental data(λ_{max} = 402.38nm) are mentioned .

4.7 Thermodynamic Properties

On the basis of vibrational analysis at B3LYP/6-311++G(d,p) level, the standard statistical thermodynamic functions: standard heat capacity (C_P), standard entropy (S), andstandard enthalpy changes (H) for the title compound were obtained from the theoretical harmonic frequencies and listed in Table 6.

Table 6.Thermodynamic properties for Chloramphenicol obtained by B3LYP/6-311++G (d,p) method.

T (K)	S (J/mol.K)	Cp (J/mol.K)	H (kJ/mol)
100	422.79	148.29	9.68
200	551.63	231.28	28.74
298.15	658.55	309.23	55.28
300	660.47	310.67	55.85
400	760.16	384.29	90.68
500	852.79	446.11	132.31
600	938.69	495.71	179.49
700	1018.19	535.33	231.12
800	1091.84	567.42	286.31
900	1160.24	593.87	344.41
1000	1223.99	615.97	404.94

To analyze the change of thermodynamic functions (heatcapacity, entropy and enthalpy) according to varying temperaturefor the title molecule, the temperature was scanned from 100 K to1000 K, in steps of 100 K due to the factthat, the molecular vibrational intensities increases with increase in temperature[37].Fromthis table, it can be observed that these thermodynamic functions are increasing with temperature. The correlation equations between heat capacities, entropies, enthalpy changes and temperatures were fitted by quadratic formulae and the corresponding fitting factors (R^2) for these thermodynamic properties are 0.99971, 0.9976and 0.99953, respectively. The corresponding fitting equations are as followsand the correlation graphics of those shown in Fig 7.

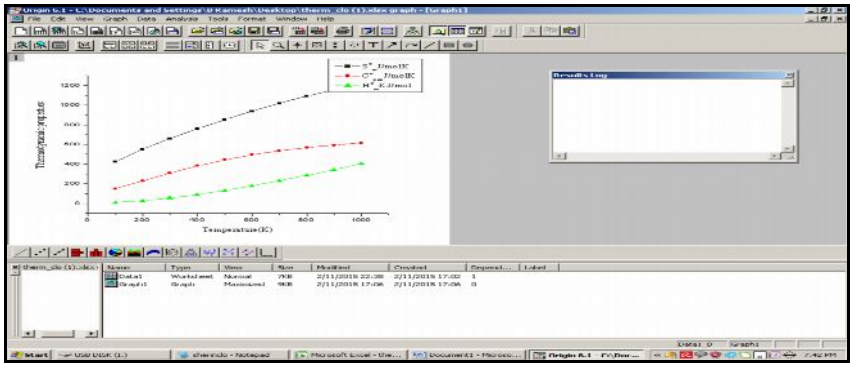

Fig 7. Correlation graphs of Thermodynamic properties at different temperature ofthe Chloramphenicol obtained by B3LYP/6-31++G(d,p) method.

The observed relations of the thermodynamic functions vs. temperatures with the regression factors(R^2) not less than 0.9995 for CLP are given by

$C_P = 50.7782 + 1.00387\ T - 4.42\times10^{-4}T^2 (R^2 = 0.99971)$
$S = 306.83384 + 1.27378\ T - 3.60867\times10^{-4}T^2 (R^2 = 0.9976)$
$H = -13.84435 + 0.16446\ T + 2.58333T\times10^{-4}T^2 (R^2 = 0.99953)$

All the thermodynamic data supply helpful information for the further study on the CLP. They can be used to compute the other thermodynamic energies according to the relationships ofthermodynamic functions and estimate directions of chemical reactions according to the second law of thermodynamics in thermo chemical field[38]. It should be kept in mind that all thermodynamic calculations were done in gas phase and they could not be used in solution.

Conclusions

FT-IR and FT-Raman spectra of 2,2-dichloro-N-[1,3-dihydroxy-1-(4-nitrophenyl)propan-2-yl were recorded and analyzed. The vibrational wavenumbers were computed using DFT with 6-311++G(d,p) basis set. The difference between the corresponding wavenumbers (observed and calculated) is very small for most of the fundamentals. Therefore, the results presented in this work for the mentioned compound indicate that this level of theory is reliable for the predictionof both infrared and Raman spectra of the title compound. The molecularorbital energy and λ_{max} of the title compound were performedand compared with an experimental and theoretical method. Other electronic structure properties such as NBO and HOMO–LUMO analysis put the lights on molecular conjugation, intermolecular stabilization, electron donor and acceptor aptitudes. The lowering of HOMO–LUMO band gap supports bioactive property of the molecule. The calculated first hyperpolarizability of the title compound is thirty five times that of standard NLO material urea and the title compound and its derivatives are attractive object for future studies of nonlinear optical properties. Furthermore, theoretical calculations gave the thermodynamic properties (heat capacity, entropy and enthalpy) for the compound. It can be observed that these thermodynamic functions are increasing with temperature ranging from 100 to 1000 K due to the fact that the molecular vibrational intensities increase with temperature. MESP plays an important role in determining stability of the molecule. The lone pair electrons which provide stabilization to the molecular structure enhance its bioactivity. This studydemonstrates that scaled calculations are powerful approach for understanding the vibrational spectra of medium sized organic compounds.

References

1. Bhutta ZA, Niazi SK, Naqvi SH, Suria A, Indian Journal of Pediatrics,1992,59, 213-19.
2. Stefanovic OD, StanojevicDD, Comic LR,Acta Pol Pharm,2012,69(3),457-63.
3. Pécoul B, Varaine F, Keita M, Soga G, Djibo A, Soula G, Abdou A, Etienne J, Rey M, The Lancet,1991,338(8771),862–866.
4. R.L. Rosenthal, A. Blackman, JAMA,1965, 191 (3), 136–137.
5. Gaussian 03 Program, Gaussian Inc., Wallingford, CT, 2004.
6. J.B. Foresman, A. Frisch, Exploring Chemistry with Electronic Structure Methods,Gaussian Inc., Pittsburgh, 1996.
7. Michał H. Jamroz, SpectrochimicaActa A, 2013,114, 220–230.

8. G. Keresztury, S. Holly, J. Varga, G. Besenyei, A.Y. Wang, J.R. Durig, Spectrochim.Acta A,1993,49, 2007–2026.
9. E.D.Glendening, A.E.Reed, J.E.Carpenter, F.Weinhold, NBO Version3.1, TCI, University of Wisconsin, Madison, 1998.
10. D.A. Kleinman, Phys. Rev 1962, 126, 1977–1979.
11. A. Atac, M. Karabacak, E. Kose, C. Karaca, Spectrochim. Acta A,2011, 83, 250–258.
12. G. Varsanyi, Assignments of Vibrational Spectra of 700 Benzene Derivatives,Wiley, New York, 1974.
13. K.B. Wiberg, A. Shrake, Spectrochim. Acta A,1973, 29, 583–587.
14. G. Varsanyi, Vibrational Spectra of Benzene Derivates, Academic Press, NewYork, 1969.
15. 15.M. Arivazhagan, V. Krishnakumar, R. John Xavier, G. Ilango, V. Balachandran,Spectrochim. Acta A,2009,72, 941–946.
16. H. Stetter, E. Rauscher, Chem. Ber.,1960,93, 2054.
17. T. Chithambarathanu, V. Umayorubaghan, V. Krishnakumar, Indian J. Pure Appl. Phys., 2003,41, 844–848.
18. G. Varsanyi, Assignments for Vibrational Spectra of Seven Hundred BenzeneDerivatives, Academic Kiacio, Budapet, 1973,vols. 1–2.
19. M. Silverstein, G. Clayton Basseler, C. Morill, Spectrometric Identification ofOrganic Compounds, Wiley, New York, 2001.
20. P.S. Kalsi, Spectroscopy of Organic Compounds, Wiley Eastern Limited,NewDelhi, 1993.
21. V.S. Madhavana, H.T. Vargheseb, S. Mathewc, J. Vinsovad, C.Y. Panicker,Spectrochim. ActaA,2009,72, 547–553.
22. V. Arjunan, I. Saravanan, P. Ravindran, S. Mohan, Spectrochim. Acta A, 2009,74, 642–649.
23. J. Chocholousova, V. Vladinuirspirko, P. Hobza, Phys. Chem.,2004,6, 37.
24. F. Weinhold, C.R. Landis, Valency and Bonding: A Natural Bond Orbital Donor–Acceptor Perspective, Cambridge University Press,New York,2005, 215–274.
25. F.J. Luque, M. Orozco, P.K. Bhadane, S.R. Gadre, J. Phys. Chem,1993,97, 9380–9384.
26. Y.X. Sun, Q.L. Hao, W.X. Wei, Z.X. Yu, L.D. Lu, X. Wang, Y.S. Wang, J. Mol. Struct.: Theochem, 2009,904, 74–82.
27. G.J. Gainsford, M.D.H. Bhuiyan, A.J. Kay, Acta. Crystallogr. Sect. E 70 (2014)029–030.
28. A. Garito, R. Shi, M. Wu, Physics Today,1994, 51-57.
29. M. Adant, M. Dupuis, J.L. Bredas, Int. J. Quantum Chem,1995,56, 497–507.
30. K. Fukui, T. Yonezawa, H. Shingu, J. Chem. Phys.,1952,20, 722.
31. S. Gunasekaran, R.A. Balaji, S. Kumeresan, G. Anand, S. Srinivasan, Can. J. Anal.Sci. Spectrosc., 2008, 53,149.
32. I. Fleming, Frontier Orbitals and Organic Chemical Reactions, John Wiley andSons, NewYork, 1976, 05–27.
33. B. Kosar, C. Albayrak, Spectrochim. Acta A,2011,78,160.
34. G. Keresztury, S. Holly, J. Varga, G. Besenyei, A.Y. Wang, J.R. Durig, Spectrochim.Acta A,1993,49, 2007–2026.
35. M.E. Casida, C. Jamorski, K.C. Casida, D.R. Salahub, J. Chem. Phys.,1998,108,4439–4449.
36. F.A. Cotton, C.W. Wilkinson, Advanced Inorganic Chemistry, third ed.,Interscience Publisher, New York, 1972.
37. Z. Ran, D. Baotong, S. Gang, S. Yuxi, Spectrochim. Acta A,2010,75,1115.
38. R. Zhang, B. Du, G. Sun, Y.X. Sun, Spectrochim. Acta A,2010,75, 1115–1124.

*****